Available online at www.sciencedirect.com
SCIENCE DIRECT®
International Journal of Heat and Mass Transfer 48 (2005) 2779–2786
International Journal of HEAT and MASS TRANSFER
www.elsevier.com/locate/ijhmt

Heat and mass transfer coefficients of falling-film absorption process

Isamu Fujita [a], Eiji Hihara [b,*]

[a] Port and Airport Research Institute, Independent Administrative Institution, 3-1-1, Nagase, Yokosuka-shi, Kanagawa 239-0826, Japan
[b] Institute of Environmental Studies, The University of Tokyo, 7-3-1, Hongo, Bunkyo-ku, Tokyo 113-0033, Japan

Received 14 April 2003; received in revised form 23 September 2004
Available online 9 April 2005

Abstract

This paper deals with the method to calculate heat and mass transfer coefficients of falling film absorption process over vertical tube or plate type surface employed in absorption refrigeration system. The conventional log mean temperature/concentration difference method is criticized for lack of physical rationality, and for incorrect results from the calculation. A new method based on a simplified model is proposed and demonstrated by numerical simulations and comparison analysis.
© 2005 Elsevier Ltd. All rights reserved.

Keywords: Falling film absorption; Heat and mass transfer coefficients; Absorption refrigeration

1. Introduction

Absorption refrigeration has been widely used in air-conditioning and refrigeration systems. Recently, much attention has been paid to a vertical-tube or plate-type absorber in order to make the system much more compact [1–3]. In absorber, as is schematically shown in Fig. 1, vapor refrigerant is absorbed into thin liquid solution film. The latent heat of vapor by the absorption is transferred from the bulk solution into the coolant through a tubular or plate surface. In the coupled heat and mass transfer process, how to reasonably define and calculate heat and mass transfer coefficients using available experimental data is still disputable. The conventional method of calculating coefficients is usually based on the temperature and the concentration values of solution measured at the inlet and outlet sides of the absorber. Due to the large variation of selection of driving force, the two calculated coefficients have obvious difference even for same experimental data, as mentioned by Islam et al. [4]. An example of the conventional method is using the log mean temperature/concentration difference, Eq. (1), such as given by Kang et al. [5].

$$\alpha_c = \frac{Q_c}{l\Delta_{lm}T} \tag{1a}$$

$$\beta = \frac{\Delta M_s}{l\Delta_{lm}X} \tag{1b}$$

while Q_c and ΔM_s are the heat transferred from the solution to the coolant and the mass of the vapor refrigerant absorbed into the solution per unit width of the heat transfer surface, respectively; l is the length of the absorber; and $\Delta_{lm}T$ and $\Delta_{lm}X$ are log mean temperature and concentration differences, respectively. The log mean

* Corresponding author. Tel./fax: +81 3 5841 6323.
E-mail address: hihara@k.u-tokyo.ac.jp (E. Hihara).

0017-9310/$ - see front matter © 2005 Elsevier Ltd. All rights reserved.
doi:10.1016/j.ijheatmasstransfer.2004.11.028

Nomenclature

C_p	specific heat capacity under constant pressure, kJ kg^{-1} K^{-1}
h	specific enthalpy, kJ kg^{-1}
l	length of the heat transfer surface, m
L	latent heat, J/kg
M	mass flow rate per unit width, kg s^{-1} m^{-1}
P	pressure, kPa
Q	heat transferred per unit width, W m^{-1}
R_{ef}	film Reynolds number, –
T	temperature, K
x	x-coordinate along the heat transfer surface, –
X	mass concentration of refrigerant in the solution, –

Greek symbols

α	heat transfer coefficient, W m^{-2} K^{-1}
β	mass transfer coefficient, kg m^{-2} s^{-1}

Subscripts

c	coolant
s	solution
v	vapor phase
*	non-dimensional

difference method is one of the most commonly used methods probably due to its simplicity. It is, however, merely a subjective analogy of the complex heat and mass transfer process to a heat exchanger model with two working fluids. Its theoretical background and accuracy are still doubtful and need further exploration. This paper, mainly targeting a vertical tube or plate-type absorber, will analyze the different methods of calculating the coefficients and reveal the defects of conventional methods. Lastly, a new method will be proposed based on a simplified model.

2. Falling film absorption

In this section, the traditional model of simple heat exchanger with two working fluids will be retrieved firstly, and then its extension to the absorber model will be given.

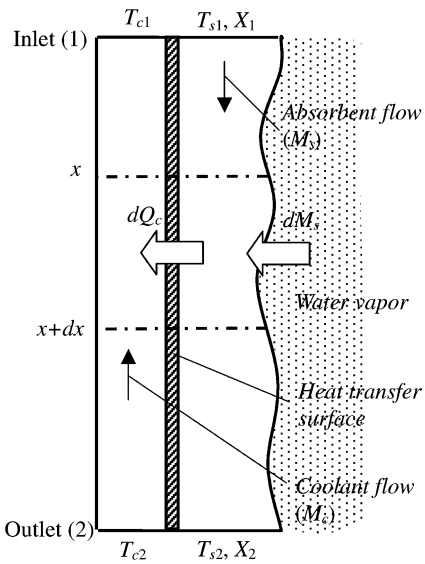

Fig. 1. Schematic of an absorber.

2.1. Simple heat exchanger model with two working fluids

The log mean temperature difference method for a heat exchanger with two working fluids is widely available in many textbooks, such as [6]. Referring to Fig. 2 and assuming constant specific heat and mass flow rate of the two involved fluids, the temperature distribution along the heat transfer surface may be described by the differential equation, Eq. (2).

$$\frac{\mathrm{d}}{\mathrm{d}x}\begin{bmatrix} T_s \\ T_c \end{bmatrix} = \begin{pmatrix} -\dfrac{\alpha}{M_s C_{p_s}} & \dfrac{\alpha}{M_s C_{p_s}} \\ -\dfrac{\alpha}{M_c C_{p_c}} & \dfrac{\alpha}{M_c C_{p_c}} \end{pmatrix} \begin{bmatrix} T_s \\ T_c \end{bmatrix} = \mathbf{A}\begin{bmatrix} T_s \\ T_c \end{bmatrix} \tag{2}$$

The vector variable $[T_s, T_c]^T$ can be decomposed into two eigenspace of the coefficient matrix $\mathbf{A}$. Letting $\boldsymbol{e}_i$ ($i = 1, 2$) be eigenvectors of $\mathbf{A}$, Eq. (2) can be written as Eq. (3).

$$\begin{bmatrix} T_s \\ T_c \end{bmatrix} = s_1\mathbf{e}_1 + s_2\mathbf{e}_2 \tag{3}$$

Each component s_i in Eq. (3) is independent of each other and satisfies Eq. (4) and (5).

$$\frac{\mathrm{d}s_i}{\mathrm{d}x} = \lambda_i s_i \quad (i = 1, 2) \tag{4}$$

$$s_i(x) = s_i(0)\exp(\lambda_i x) \tag{5}$$

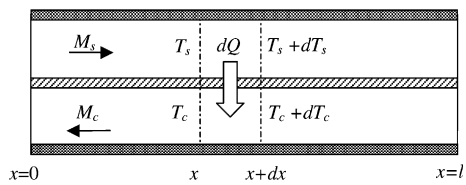

Fig. 2. Heat transfer model for a simple counter current heat exchanger.

where λ_i ($i = 1,2$) are eigenvalues of the matrix $\mathbf{A}$. Using the boundary condition at $x = 0$ and l, the integration of Eq. (5) gives Eq. (6).

$$Q = M_s C_{p_s}(T_s(0) - T_s(l)) = M_c C_{p_c}(T_c(0) - T_c(l)) \tag{6a}$$

$$(T_s(l) - T_c(l)) = (T_s(0) - T_c(0)) \exp\left[\frac{\alpha l}{Q}\{(T_s(0) - T_s(l)) - (T_c(0) - T_c(l))\}\right] \tag{6b}$$

Eq. (6a) is the heat conservation and Eq. (6b) expresses the heat transfer rate. From Eq. (6b), the heat transfer coefficient α can be solved explicitly.

$$\alpha = \frac{Q}{l\Delta_{\mathrm{lm}}T} \tag{7}$$

while $\Delta_{\mathrm{lm}}T$ is the log mean temperature difference given by Eq. (8).

$$\Delta_{\mathrm{lm}}T = \frac{\{(T_s(l) - T_c(l)) - (T_s(0) - T_c(0))\}}{\ln\left(\frac{T_s(l)-T_c(l)}{T_s(0)-T_c(0)}\right)} \tag{8}$$

It is known from Eq. (8) that, for a simple heat exchanger, the control equation may be easily integrated by decomposing the state variable $[T_s, T_c]^{\mathrm{T}}$ into the eigenspaces of the equation, and the log mean temperature difference expression is thus obtained.

2.2. Adiabatic film absorption

For adiabatic absorption process, as illustrated in Fig. 3, a log mean difference is approximately valid. Eqs. (9)–(11) may describe the physical model of the adiabatic absorption.

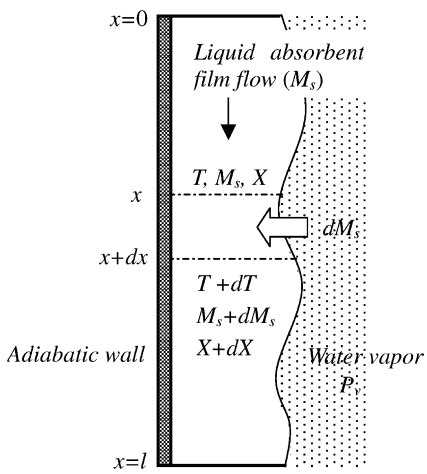

Fig. 3. Absorption model for an adiabatic absorber.

$$\mathrm{d}M_s = \beta\{P_v - P(X,T)\}\,\mathrm{d}x \tag{9}$$

$$\mathrm{d}T_s = \frac{L}{M_s C_{p_s}}\mathrm{d}M_s \tag{10}$$

$$\mathrm{d}X = \frac{1-X}{M_s}\mathrm{d}M_s \tag{11}$$

Eq. (9) assumes that the absorption rate from the vapor refrigerant into the solution is proportional to the pressure difference. Eqs. (10) and (11) are heat and mass conservation, respectively. The equilibrium pressure of the solution is defined as the saturated vapor pressure of the solution at the concentration X and the temperature T, and may be Taylor-expanded as Eq. (12).

$$P(X,T) = P_v + \frac{\partial P}{\partial X}(X - X_v) + \frac{\partial P}{\partial T}(T - T_v) \tag{12}$$

while X_v and T_v can be chosen arbitrarily at a certain state while the corresponding saturated vapor pressure is P_v. Allowing $X - X_v$ and $T - T_v$ to be referred as X and T again, respectively, Eqs. (9)–(12) can be transformed into a matrix form as Eq. (13).

$$\frac{\mathrm{d}}{\mathrm{d}x}\begin{bmatrix} X \\ T \end{bmatrix} = \beta\begin{pmatrix} -\eta_X\frac{\partial P}{\partial X} & -\eta_X\frac{\partial P}{\partial T} \\ -\eta_T\frac{\partial P}{\partial X} & -\eta_T\frac{\partial P}{\partial X} \end{pmatrix}\begin{bmatrix} X \\ T \end{bmatrix} = \mathbf{A}\begin{bmatrix} X \\ T \end{bmatrix} \tag{13}$$

while parameters in Eq. (13) are defined by Eq. (14).

$$\eta_X = \frac{1-X}{M_s} = \frac{X_s(l) - X_s(0)}{\Delta M_s}, \quad \eta_T = \frac{L}{M_s C_{p_s}} = \frac{T_s(l) - T_s(0)}{\Delta M_s} \tag{14}$$

By the same way as used in the previous section, the state variable may be decomposed into the eigenspace of $\mathbf{A}$, which has an eigenvalue and its component as Eq. (15).

$$\lambda = -\beta\left(\eta_X\frac{\partial P}{\partial X} + \eta_T\frac{\partial P}{\partial T}\right) = -\frac{\beta}{\Delta M_s}\left\{(X(l) - X(0))\frac{\partial P}{\partial X} + (T_s(l) - T_s(0))\frac{\partial P}{\partial T}\right\}$$
$$s = \frac{\partial P}{\partial X}X + \frac{\partial P}{\partial T}T \tag{15}$$

The component s in Eq. (15) obeys also Eq. (5) and has an integration.

$$\left(\frac{\partial P}{\partial X}X(l) + \frac{\partial P}{\partial T}T(l)\right) = \left(\frac{\partial P}{\partial X}X(0) + \frac{\partial P}{\partial T}T(0)\right)\exp\left[-\frac{\beta l}{\Delta M_s}\left\{(X(l) - X(0))\frac{\partial P}{\partial X} + (T_s(l) - T_s(0))\frac{\partial P}{\partial T}\right\}\right] \tag{16}$$

Consequently, the total mass absorbed into the solution ΔM_s is expressed by Eq. (17).

$$\Delta M_s = -\beta l \frac{\left\{(X(l)-X(0))\frac{\partial P}{\partial X} + (T(l)-T(0))\frac{\partial P}{\partial T}\right\}}{\ln\left(\frac{\partial P}{\partial X}X(l)+\frac{\partial P}{\partial T}T(l)\right)/\left(\frac{\partial P}{\partial X}X(0)+\frac{\partial P}{\partial T}T(0)\right)} = \beta l \frac{\Delta P(l)-\Delta P(0)}{\ln(\Delta P(l)/\Delta P(0))} = \beta l \Delta_{\mathrm{lm}} P \tag{17}$$

while $\Delta P(x) = P_v - P(X(x), T(x))$. Eq. (17), identical to Eq. (1b), shows the final form of the mass transfer.

2.3. Falling film absorber

In this section, an absorption process as displayed in Fig. 1 is discussed. The heat balance at an infinitesimal domain in the solution is assumed to be

$$L\mathrm{d}M_s = M_s \frac{\partial h_s}{\partial X}\mathrm{d}X + M_s \frac{\partial h_s}{\partial T_s}\mathrm{d}T_s + \mathrm{d}Q_c \tag{18}$$

For the mass balance in the solution, Eq. (11) is used again here. The heat balance in the coolant is given by Eq. (19).

$$M_c C_{p_c} \mathrm{d}T_c = -\mathrm{d}Q_c \tag{19}$$

Here, the mass flux is assumed to be in proportion to the chemical potential difference between the solution and the vapor refrigerant. So the mass transfer equation is expressed as Eq. (20).

$$\mathrm{d}M_s = \beta\{\ln P_v - \ln P_s(X, T_s)\}\mathrm{d}x \tag{20}$$

Applying Taylor expansion to the term of $\ln P_s$, we have Eq. (21).

$$\ln P_s(X, T_s) = \ln P(X_1, T_{s2}) + \frac{\partial \ln P_s}{\partial X}(X - X_1) + \frac{\partial \ln P_s}{\partial T_s}(T_s - T_{c2}) \tag{21}$$

The mass transfer rate equation can be rewritten as Eq. (22).

$$\mathrm{d}M_s = \beta\left\{\Delta \ln P - \frac{\partial \ln P_s}{\partial X}(X - X_1) - \frac{\partial \ln P_s}{\partial T_s}(T_s - T_{c2})\right\}\mathrm{d}x \tag{22}$$

while $\Delta \ln P$ stands for $\ln P_v - \ln P(X_1, T_{s2})$. Eq. (23) is heat transfer from solution to coolant.

$$\mathrm{d}Q = \alpha(T_s - T_c)\mathrm{d}x \tag{23}$$

By introducing non-dimensional variables, Eq. (11) and Eq. (18)–(23) yield the governing equation like Eq. (24).

$$\frac{\mathrm{d}}{\mathrm{d}x^*}\left[\mathrm{d}X^* \quad \mathrm{d}T_s^* \quad \mathrm{d}T_c^*\right]^{\mathrm{T}} = \left[\frac{\alpha_a^*}{H_L} \quad \left(1-\frac{H_X}{H_L}\right)\alpha_a^* \quad 0\right]^{\mathrm{T}} + \begin{pmatrix} -\frac{\alpha_a^*}{H_L} & -\frac{\alpha_a^*}{H_L} & 0 \\ -\frac{1}{H_T}\left(1-\frac{H_X}{H_L}\right)\alpha_a^* & -\frac{1}{H_T}\left(1-\frac{H_X}{H_L}\right)\alpha_a^* - \frac{\alpha_c^*}{H_T} & \frac{\alpha_c^*}{H_T} \\ 0 & -\alpha_c^* & \alpha_c^* \end{pmatrix} \times \begin{bmatrix} X^* \\ T_s^* \\ T_c^* \end{bmatrix} \tag{24}$$

while $H_L = \left(\frac{M_s \Delta X}{1-X}L\right)/\left(M_c C_{p_c}\Delta T\right)$ is non-dimensional latent heat,

$H_T = \left(M_s \frac{\partial h_s}{\partial T_s}\Delta T\right)/(M_c C_{p_c}\Delta T)$ is non-dimensional specific heat capacity,
$H_X = \left(M_s \frac{\partial h_s}{\partial X}\Delta X\right)/\left(M_c C_{p_c}\Delta T\right)$ is non-dimensional heat of dilution,
$\alpha_c^* = \alpha l \frac{1}{M_c C_{p_c}}$ is non-dimensional heat transfer coefficient,
$\alpha_a^* = \beta l \frac{L}{M_c C_{p_c}} \frac{\Delta(\ln P)}{\Delta T}$ is non-dimensional mass transfer coefficient.

$$T^* = (T - T_{c2})/\Delta T \quad X^* = (X - X_1)/\Delta X \tag{25}$$

The non-dimensional variables of T and X are defined by Eq. (25). ΔT and ΔX are scaling factors for temperature and concentration respectively whose definitions are given in Fig. 4. The term of $\Delta(\ln P)/\Delta T$ in the mass transfer coefficient converts the pressure-based coefficient into temperature scale. Fig. 4 illustrates a schematic of the absorption process on X–T chart. If the solution in the absorber is at point A, the driving force for the absorption can be expressed by the length of segment AC in temperature scale. On the other hand, the driving force for the heat transfer corresponds to the

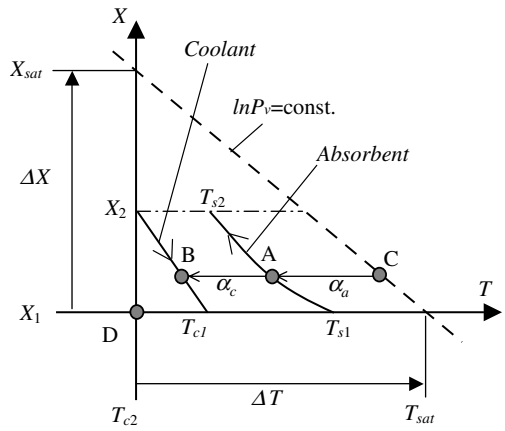

Fig. 4. Schematics of absorption process on T–X chart.

segment AB. If the heat generation by the absorption and the heat transfer to the coolant are balanced, the ratio of α_a^* to α_c^* is obtained by the schematic relation of BA:AC $= 1/\alpha_a^* : 1/\alpha_a^*$ in non-dimensional form. The heat and mass transfer coefficients from the experimental data determine α_a and α_c, and thus the integration of the governing Eq. (24) satisfies the two point boundary conditions measured at the inlet and outlet. Although an explicit integration of (24) may be possible, it requires tedious calculation, and thus numerical calculation or some approximation is more practical. A finite difference method or a shooting method is suitable for the numerical. In this study, the latter method, including Runge–Kutta method for integrating and Simplex method [7] for fitting boundary conditions, is used for the calculation of typical experimental data obtained by the authors. Fig. 5 gives the non-dimensional temperature and concentration profiles in the absorber. From Fig. 5a, it may be noted that the temperature of the solution changes much more drastically than other properties.

2.4. Simplified method for calculating heat and mass transfer coefficients

The heat and mass transfer equations are shown in Eq. (26) and (27).

$$dQ_a = \alpha_a(T_v(x) - T_s(x))dx \tag{26}$$

$$dQ_c = \alpha_c(T_s(x) - T_c(x))dx \tag{27}$$

while $T_v(x)$ is the interfacial equilibrium temperature, calculated using vapor pressure and bulk solution concentration, i.e. point C in Fig. 4. For the heat balance of solution, Eq. (28) is given.

$$M_s\left(\frac{\partial h_s}{\partial T_s}dT_s + \frac{\partial h_s}{\partial X}dX\right) = dQ_a - dQ_c \tag{28}$$

By non-dimensional transformation, Eq. (29) is obtained from Eq. (28).

$$\frac{dT_s^*}{dx^*} = \alpha_a^*(T_v^* - T_s^*) - \alpha_c^*(T_s^* - T_c^*) - N_{XT} \tag{29}$$

$$N_{XT} = \left(\frac{\partial h_s}{\partial X}\Delta X\frac{dX^*}{dx^*}\right)\Big/\left(\frac{\partial h_s}{\partial T_s}\Delta T\right),$$

$$\alpha_a^* = \frac{l}{M_s C_{p_s}}\alpha_a, \quad \alpha_c^* = \frac{l}{M_s C_{p_s}}\alpha_c \tag{30}$$

As shown in Fig. 6 and given in Eqs. (31)–(33), a linear distribution along the flow direction is specially assumed for solution concentration, coolant temperature, and solution equilibrium temperature, respectively.

$$X^*(x^*) = X^*(1)x^* \tag{31}$$

$$T_c^*(x^*) = T_c^*(0)(1 - x^*) \tag{32}$$

$$T_v^*(x^*) = 1 - X^*(1)x^* \tag{33}$$

By substituting Eqs. (31)–(33) into Eq. (29) and further integrating, Eq. (34) may be obtained.

$$T_s^*(x^*) - T_{eq}^*(x^*) = \left(T_s^*(0) - T_{eq}^*(0)\right)\exp(-\alpha^* x^*) \tag{34}$$

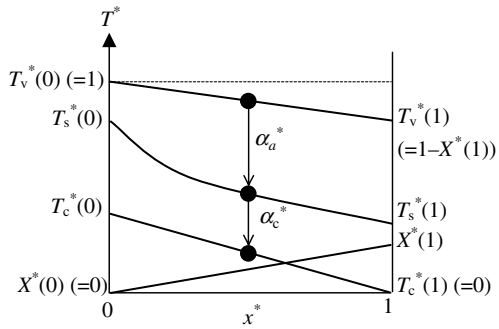

Fig. 6. Simplified model for calculating absorption coefficient α_a^* and heat transfer coefficient α_c^*.

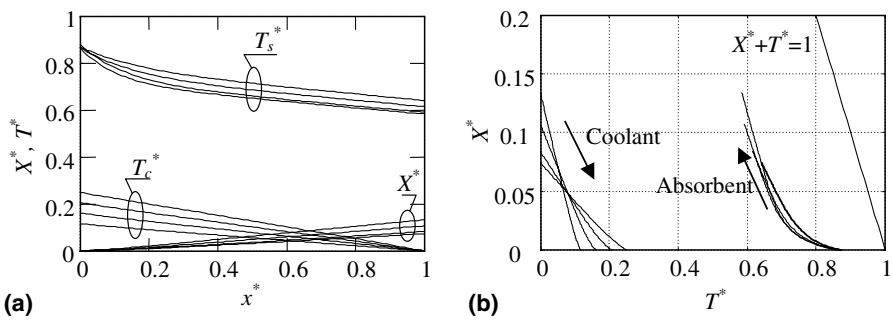

Fig. 5. Temperature and concentration distributions in an absorber on $X^*/T^* - x^*$ chart (a) and $T^* - X^*$ chart (b). Experimental results were fitted to Eq. (24) using Simplex method. The experiment was carried out using a flat surface of 1 m in length inclined in 45° under the following conditions; X_1 = 38 wt.%(H_2O), T_{s1} = 60 °C, T_{c2} = 30 °C, M_s = 0.4–1.5 × 10 $^{-1}$ kg/ms, M_c = 5.0 × 10 $^{-1}$ kg/ms.

From Eq. (34), it may be seen that, with $\alpha^* x^* \to \infty$ the temperature of the solution $T_s^*(x^*)$ approaches to equilibrium temperature T_{eq}^* as displayed in Eq. (35).

$$T_{eq}^*(x^*) = \gamma T_v^*\left(x^* - \frac{1}{\alpha^*}\right) + (1-\gamma)T_c^*\left(x^* - \frac{1}{\alpha^*}\right) - \frac{N_{XT}}{\alpha^*} \tag{35}$$

while $\alpha^* = \alpha_a^* + \alpha_c^*$, and $\gamma = \alpha_a^*/\alpha^*$. If the heat of dilution is relatively small or α^* is very large, the last term in Eq. (35) can be neglected, T_{eq}^* is reduced to a simpler expression.

Applying the boundary conditions, Eq. (34) and (35) yield an explicit expression of γ in Eq. (36).

$$\gamma = \frac{\left\{T_s^*(1) - T_c^*\left(1-\frac{1}{\alpha^*}\right)\right\} - \left\{T_s^*(0) - T_c^*\left(-\frac{1}{\alpha^*}\right)\right\}e^{-\alpha^*} + \frac{N_{XT}}{\alpha^*}(1-e^{-\alpha^*})}{\left\{T_v^*\left(1-\frac{1}{\alpha^*}\right) - T_v^*\left(-\frac{1}{\alpha^*}\right)e^{-\alpha^*}\right\} - \left\{T_c^*\left(1-\frac{1}{\alpha^*}\right) - T_c^*\left(-\frac{1}{\alpha^*}\right)e^{-\alpha^*}\right\}} \tag{36}$$

In order to determine the magnitude of α^* the heat acquired by the coolant is considered in Eq. (37). With further transformation, Eq. (38) is obtained from Eq. (37).

$$T_c^*(0) = H_T\alpha_c^*\int_0^1 \left(T_s^*(x^*) - T_c^*(x^*)\right)dx^* \tag{37}$$

$$T_c^*(0) = H_T\gamma(1-\gamma)\alpha^* P(\alpha^*, \gamma) \tag{38}$$

$$P(\alpha^*, \gamma) = 1 - \frac{X^*(1)}{2} + \frac{X^*(1)}{\alpha^*} - T_c^*(0)\left(\frac{1}{2} - \frac{(1-\gamma)}{\gamma\alpha^*}\right) - \frac{N_{XT}}{\gamma\alpha^*} + \frac{1-e^{-\alpha^*}}{\gamma\alpha^*}\left(T_s^*(0) - T_{eq}^*(0)\right) \tag{39}$$

From Eq. (36) and (38), α^* and γ can be solved iteratively. Moreover, in a particular case while α^* is far larger than unity, the terms $1/\alpha^*$ can be neglected in (36) and (38), more simplified expressions of α^* and γ are obtained as given in Eqs. (40), (41).

$$\gamma = \frac{T_s^*(1) - T_c^*(1)}{T_v^*(1) - T_c^*(1)} = \frac{T_s^*(1)}{1 - X^*(1)} \tag{40}$$

$$\alpha^* = \frac{T_c^*(0)}{H_T\gamma(1-\gamma)\left\{1 - \frac{X^*(1)}{2} - \frac{T_c^*(0)}{2}\right\}} \tag{41}$$

By multiplying $\gamma(1-\gamma)$, Eq. (41) may be changed to Eq. (42).

$$\alpha^*\gamma(1-\gamma) = \frac{1}{\frac{1}{\alpha_a^*} + \frac{1}{\alpha_c^*}} = \left(\frac{T_c^*(0)}{H_T}\right)\Big/\left\{1 - \frac{X^*(1)}{2} - \frac{T_c^*(0)}{2}\right\} \tag{42}$$

Eq. (42) is analogous to the overall heat transfer coefficient.

3. Results and discussion

Comparison among involved methods is given in Fig. 7. The calculation was made by firstly assuming certain α^* and γ, secondly determining the temperature and concentration profiles numerically using (24), and then calculating α^* and γ again with the conventional model and the new model. The result by the conventional method by Eq. (1) is denoted by ○, and the result by the new method is denoted by △ in Fig. 7. Another symbol, □, represents the result by the conventional arithmetically-averaged method, as given in Eq. (43).

$$\alpha_a = \frac{Q_a}{l(T_v(l) - T_s(l) + T_v(0) - T_s(0))/2} \tag{43a}$$

$$\alpha_c = \frac{Q_c}{l(T_s(l) - T_c(l) + T_s(0) - T_c(0))/2} \tag{43b}$$

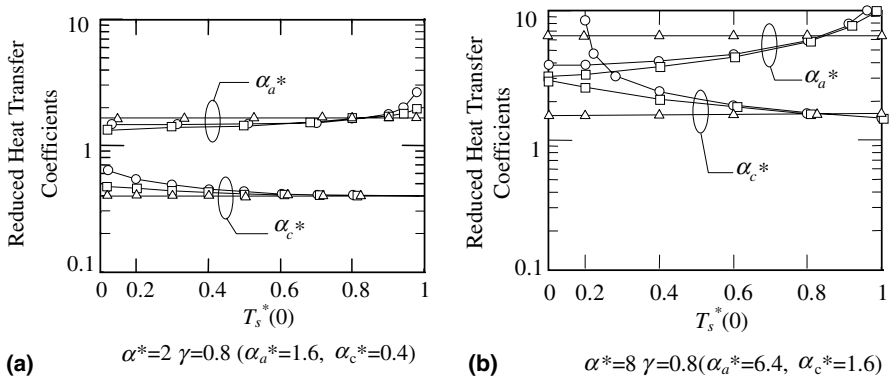

Fig. 7. Comparison of heat transfer coefficients among various methods in case of total heat transfer coefficient relatively small (a) and relatively large (b). Symbols in the figure indicate the methods of calculation; (○) is a conventional method using logarithmic mean temperature difference, (□) is a method with a mere mean value instead of a logarithmic mean value and (△) is the newly introduced method by Eq. (36) and (38).

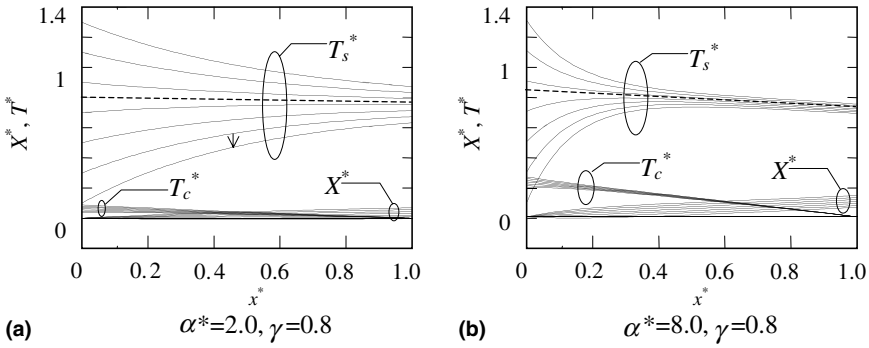

Fig. 8. Temperature and concentration profile in an absorber in case that the total heat transfer coefficient α^* is relatively small (a) and relatively large (b).

In Fig. 7, two examples are given. One is for relatively small α^* in Fig. 7a, another is for relatively large α^* in Fig. 7b. From Fig. 7, the results from the two conventional methods display obvious deviations from the reasonable values except at the neighborhood of $T_s^* = 0.8$. The deviation becomes larger with the increase of α^*. This is caused by the selection of equilibrium temperatures in the conventional methods. The conventional method hypothetically decomposes the absorption process into two independent processes: one is the heat transfer from the solution to the coolant, and the other is the absorption of refrigerant from the vapor phase to the solution. Therefore, the conventional method generally brings wrong results except the condition when the temperature of the solution changes linearly in the absorber. There are two cases for this condition, one is that the inlet temperature $T_s^*(0)$ coincides with $T_{eq}^*(0)$, and the other is the case that α^* is very small. Actually, referring to dashed lines in Fig. 8, the solution temperature profile tends to be almost linear when $T_s^*(0)$ is greater than 0.8. On the contrary, the new iterative method introduced in Section 2.4 always gives reasonable α_a^* and α_c^* regardless of the variation of $T_s^*(0)$ and α^*. Fig. 9 is an example to show the heat and mass transfer coefficients calculated by different methods. The numerical calculation and the newly introduced simplified method give almost same coefficients. Although the new method also requires an iterative calculation to solve Eq. (36) and Eq. (38), it is far easier for implement than the numerical iteration calculation to directly solve Eq. (24). If α^* is large enough, Eq. (40) and Eq. (41) can give approximate results without iteration. Additionally, it is important to know the deficiency of the conventional methods instead of accepting them without hesitation.

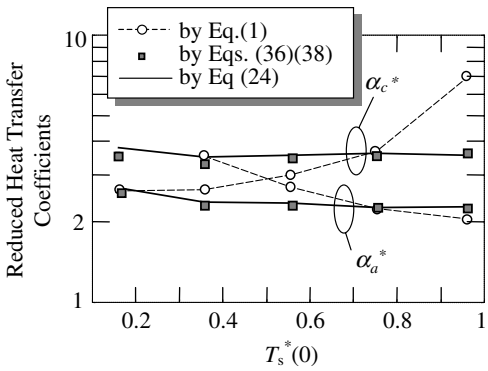

Fig. 9. Heat transfer coefficients calculated in various ways using experimental data. Experiments were carried out with 62 wt.% solution without surfactants under the conditions of Re_f = 146, P_v = 10 Torr (= 1.33 kPa), T_{c2} = 31 °C, M_c = 0.5 kg/ms and l = 1.0 m.

4. Concluding remarks

This paper discussed the methods to calculate heat and mass transfer coefficients. Compared with the direct numerical calculation, the defect of the conventional method using log mean temperature/concentration differences was revealed. Under the assumption of linear distribution of the coolant temperature, solution concentration and interfacial equilibrium temperature, a new simplified method was proposed and has been demonstrated to present good results by numerical simulation.

References

[1] E. Hihara, T. Saito, Effect of surfactant on falling film absorption, Int. J. Refrig. 16 (6) (1993) 339–436.
[2] J.K. Kwang, S.B. Neil, D.W. Byard, The interfacial turbulence in falling film absorption: effects of additives, Int. J. Refrig. 19 (5) (1996) 322–330.
[3] J.D. Killion, S. Garimella, A critical review of models of coupled heat and mass transfer in falling film absorption, Int. J. Refrig. 24 (8) (2001) 755–797.

[4] M.R. Islam, N.E. Wijeysundera, J.C. Ho, Evaluation of heat and mass transfer coefficients for falling-films on tubular absorbers, Int. J. Refrig. 26 (2) (2003) 197–204.
[5] Y.T. Kang, A. Akisawa, T. Kashiwagi, Experimental correlation of combined heat and mass transfer for NH_3–H_2O falling film absorption, Int. J. Refrig. 22 (4) (1999) 250–262.
[6] J.P. Holman, Heat Transfer, sixth ed., McGraw-Hill, 1963, pp. 536–544.
[7] W.H. Press, S.A. Teukolsky, W.T. Vetterling, B.P. Flannery, Numerical Recipes in C, Cambridge University Press, 1988.